Supplement to CAN-23-3804-ATR1 "An Alternatively Spliced Gain-of-Function NT5C2 Isoform Contributes to Chemoresistance in Acute Lymphoblastic Leukemia" (Manuel Torres-Diz et al)

Supplemental Materials and Methods

RNA-seq analysis. RNA-seq reads were first trimmed to remove adapters (BBTools version 38.87) and were then aligned using STAR version 2.7.3a to the hg38 reference genome, while providing known gene isoforms through the GENCODE annotation version 32. Additionally, we used STAR flags "--quantMode GeneCounts" and "--alignSJoverhangMin 8" to quantify genes and ensure spliced reads had an overhang of at least 8 bases. Junction spanning reads were obtained from the STAR "*_SJ.out.tab" result files and each entry was normalized by dividing by the total number of junction-spanning reads and multiplying by a factor of one million, yielding a JPM value. Visualization and downstream analyses were conducted in R using the ggplot2 and tidyverse packages.

Mutation analysis. Relapse-specific variant discovery was done using the Genome Analysis Toolkit (GATK) version 4.4.0.0 (RRID:SCR_001876) on the RNA-seq data. Shortly, aligned reads were marked for duplicated events using Picard Tools version 3.0.0. Reads spanning splicing events were split into independent reads with the SplitNCigarReads tool followed by base recalibration. To specifically call mutations that are enriched in the relapsed samples, the Mutect2 algorithm was applied using the corresponding diagnostic sample to each relapsed file in the –normal flag. All the variants were annotated using the Funcotator tool with the hg38 somatic annotation from the FuncotatorDataSourceDownloader. All the maf files from the 48 patients were loaded into the R package maftools for variant visualization and downstream analysis.

qRT-PCR. Total RNA was isolated using Maxwell RSC simplyRNA Cells kit with the Maxwell RSC48 Instrument (Promega) and reverse-transcribed using SuperScript IV (Invitrogen; 18090010). Primers used for mRNA isoform quantification are listed in Supplementary Tables. qRT-PCR was performed using PowerSYBR Green PCR Master Mix (Life Technologies). Reactions were performed on an Applied Biosystems Viia7 machine and analyzed with Viia7 RUO software (Life Technologies). When indicated, individual PCR products were gel-purified (QIAquick Gel Extraction Kit; Qiagen) and Nanopore sequenced.

Western blotting. For the Western blotting, cells were lysed in RIPA buffer plus protease and phospatase inhibitor and benzonase. 30ug of protein were loaded on NuPAGE gels. For detection by Western blotting, the following primary antibodies were used: anti-NT5C2 antibody (Sigma-Aldrich Cat# WH0022978M2, RRID:AB_1842747), anti-FPGS antibody (Abcam Cat# ab184564 [clone EPR11064], RRID:unknown), anti-CREBBP (Cell Signaling Technology Cat# 7389, RRID:AB_2616020), anti-histone H3 acetyl K9 + K14 + K18 + K23 + K27 (Abcam Cat# ab47915, RRID:AB_873860), anti-histone H3 acetyl K27 (Cell Signaling Technology Cat# 8173, RRID:AB_10949503), and anti-histone H3 (Active Motif Cat# 61475, RRID:AB_2687473) in combination with anti-rabbit or anti-mouse HRP-linked secondary antibodies (Cell Signaling Technology) and Amersham's enhanced chemiluminescence Western blotting detection reagent (GE Life Sciences). Additionally, a horseradish peroxidase-conjugated antibody was used to detect the β-actin loading control (Cell Signaling Technology Cat# 12262, RRID:AB_2566811).
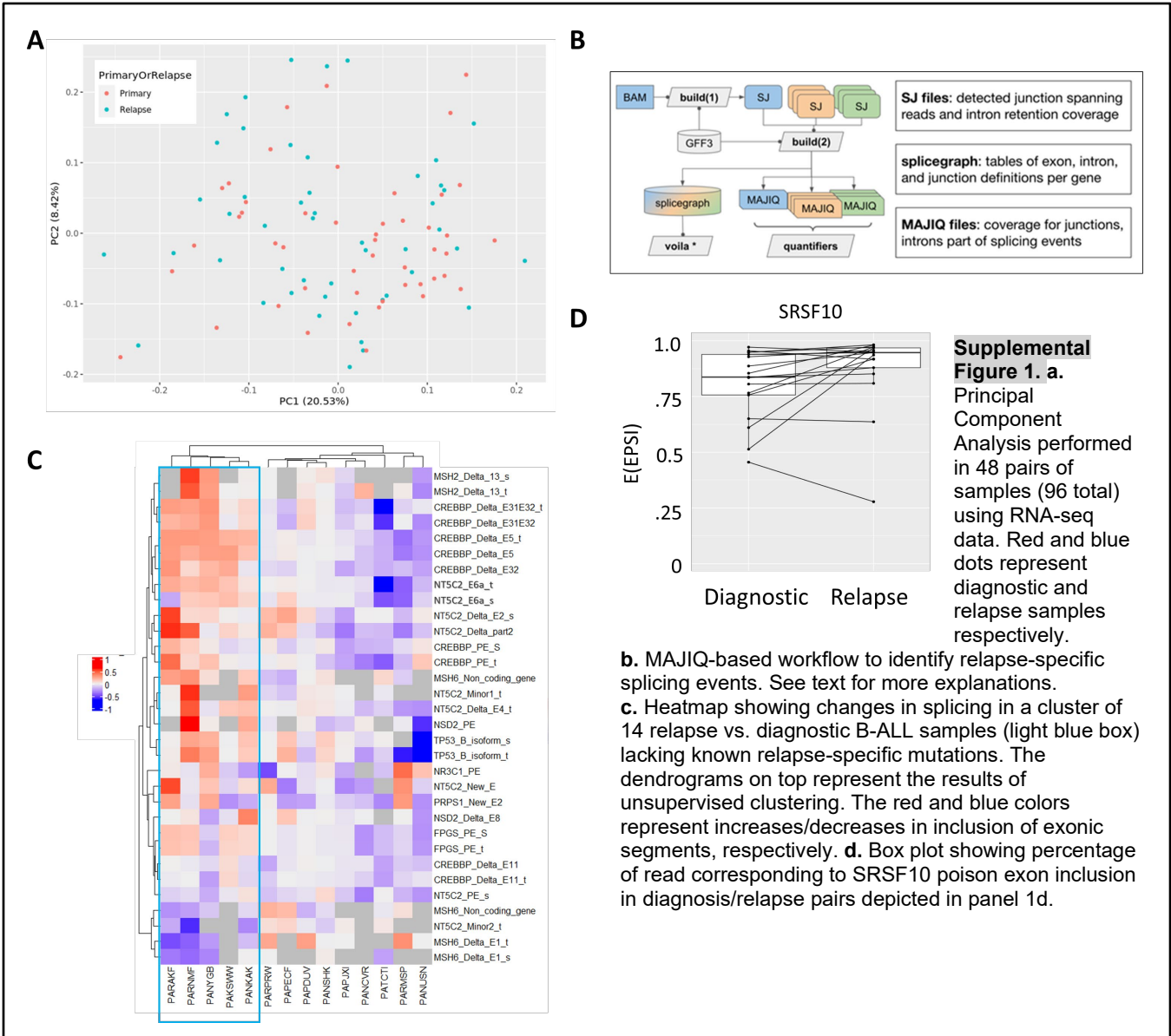
PCR and Sequencing Primers

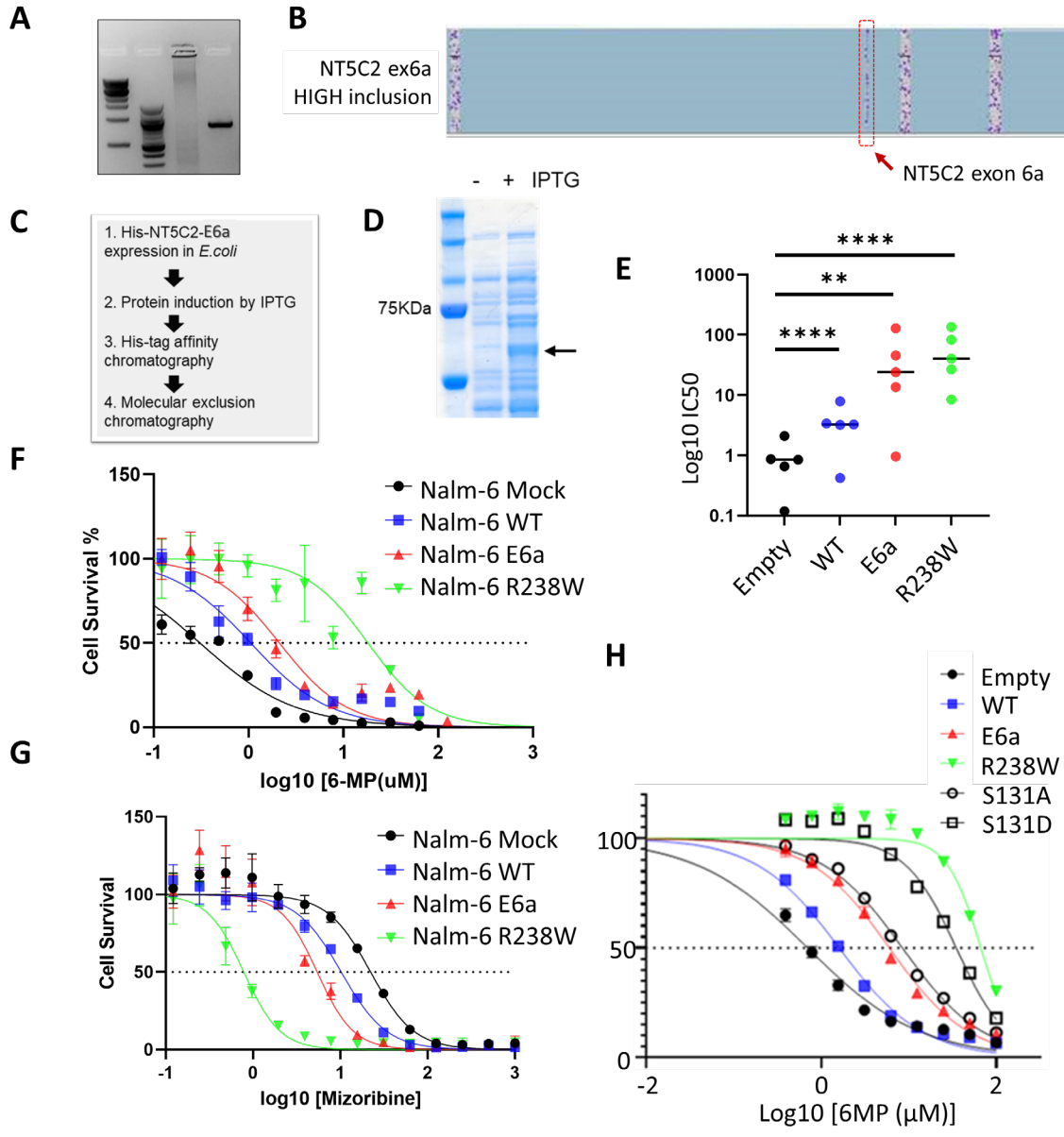| Primer_Name	Sequence
GAPDH_qPCR_F	ATGGGGAAGGTGAAGGTCG
GAPDH_qPCR_R	GGGGTCATTGATGGCAACAATA
ACTB_qPCR_F	AGCATCCCCCAAAGTTCAC
ACTB_qPCR_R	AAGGGACTTCCTGTAACAACG
NT5C2_qPCR_E4E4a_F1	TTCCCTACCAGGGGACTTGT
NT5C2_qPCR_E4E4a_R1	GAACAGCTACCTGAGAACCCC
NT5C2_qPCR_E4E4a_F2	ACATTCCCTACCAGGGGACT
NT5C2_qPCR_E4E4a_R2	ACAGCTACCTGAGAACCCCTT
NT5C2_qPCR_TOTAL_F1	CGCACAGGAGCTACATGTCT
NT5C2_qPCR_TOTAL_R1	TGGAACTGATGTCTGGACGC
NT5C2_qPCR_TOTAL_F2	CAAAGAAACGGCAAGGGTGG
NT5C2_qPCR_TOTAL_R2	TGCTTGTAGAGTTCAGCCAAGA
NT5C2_qPCR_E4E5_F1	AACTTTATAAGGGGACCAGAAACT
NT5C2_qPCR_E4E5_R1	CTAGGCAGGCCAACAGGTAG
NT5C2_qPCR_E4E5_F2	GGGGACCAGAAACTAGAGAACA
NT5C2_qPCR_E4E5_R2	CTAGGCAGGCCAACAGGTAG
NT5C2_cloning_F	ATGTCAACCTCCTGGAGTGATC
NT5C2_cloning_R	TTGTTCCTGTGAGTCCTGCC
NT5C2_E4a_cloning_F	TTCTCAGGTAGCTGTTCAGAAGAGACCAGAAACTAGAGAACAGTATCCAA
NT5C2_E4a_cloning_R	CTCTTCTGAACAGCTACCTGAGAACCCCTTATAAAGTTAAATCCATGTGC
NT5C2_R238W_cloning_F	GCTTCTGAGCtGGATGAAGGAAGTAGGGAAAGTATTTCTT
NT5C2_R238W_cloning_R	CCTTCATCCaGCTCAGAAGCAAAGGCAGTTTTCCATCTTT
FPGS_NANOPORE_F	GGGGCTTATGACTGCACCAA
FPGS_NANOPORE_R	CTTCGTCCAGGTGGTTCCAG

sgRNA for Genome Editing

sgRNA_Name	Sequence
sgRNA_Exon26_downstream	GTTTACCATGAGATCCTTAT
sgRNA_Exon26_upstream	AGAAATGTACACACGCCTGT
sgRNA_Exon25_downstream	AACTACCTCGTGTTTGGAGG
sgRNA_Exon25_upstream	CCAGAGCCGGACATTTACAA

Supplemental Figures

A

B

SJ files: detected junction spanning reads and intron retention coverage

splicegraph: tables of exon, intron, and junction definitions per gene

MAJIQ files: coverage for junctions, introns part of splicing events

C

D

SRSF10

Supplemental Figure 1. a. Principal Component Analysis performed in 48 pairs of samples (96 total) using RNA-seq data. Red and blue dots represent diagnostic and relapse samples respectively.

b. MAJIQ-based workflow to identify relapse-specific splicing events. See text for more explanations.

c. Heatmap showing changes in splicing in a cluster of 14 relapse vs. diagnostic B-ALL samples (light blue box) lacking known relapse-specific mutations. The dendrograms on top represent the results of unsupervised clustering. The red and blue colors represent increases/decreases in inclusion of exonic segments, respectively. **d.** Box plot showing percentage of read corresponding to SRSF10 poison exon inclusion in diagnosis/relapse pairs depicted in panel 1d.

Supplemental Figure 2. The role of NT5C2ex6a in chemoresistance in vitro. a. RT-PCR amplification of the full-length NT5C2ex6a cDNA from MHH-CALL4 cells. **b**. Targeted long-read ONT sequencing of the NT5C2ex6a. **c.** General schema of NT5C2 ex6a protein purification. **d.** Electrophoretic detection of the NT5C2 ex6a isoform (arrow) following induction by IPTG. **e.** Average IC50 values from 5 independent experiments depicted in Figure 3e. Asterisks indicate statistical significance per Student's t-test. **f.** The IC_{50} plot representing survival of NT5C2-expressing Nalm6 cells exposed to increasing concentrations of 6-MP. **g.** The IC_{50} plot representing survival of NT5C2-expressing Nalm6 cells exposed to increasing concentrations of mizoribine. **h.** The IC_{50} plot representing survival of additional NT5C2 variant-expressing REH cells exposed to increasing concentrations of 6-MP.
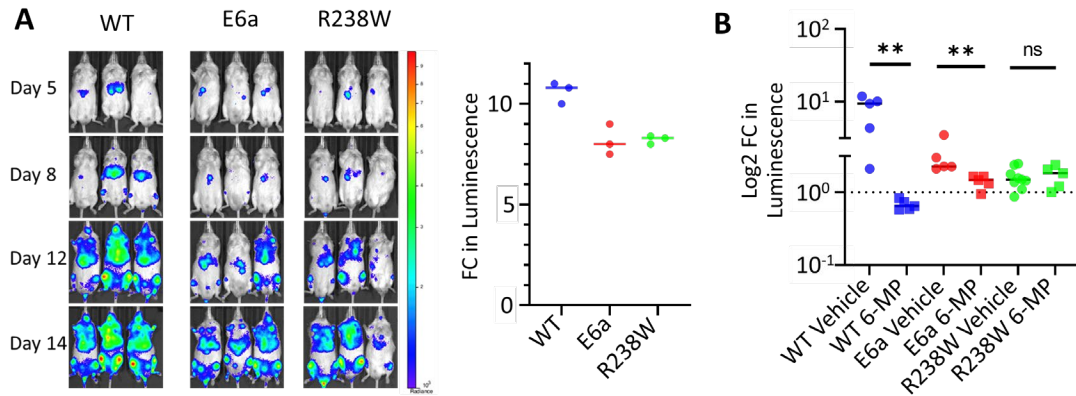
Supplemental Figure 3. The role of NT5C2ex6a in chemoresistance in vivo. a. LEFT: Ivis bioluminescence image of mice engrafted with REH Luc NT5C2 WT, E6a or R238W cells at the indicated time points. RIGHT: Quantitation of data from the previous panel, expressed as fold change in photon counts between d14 and d5. **b.** Quantitation of data from Figure 3g, expressed as fold change in photon counts between d14 and d10. Asterisks indicate statistical significance per Student's t-test.